

measurements for six substituted imidazole complexes of Fe<sup>III</sup>TPP, these investigators found  $V/\Delta$  to be nearly constant,  $0.65 \pm 0.02$ . The results from crystalline and frozen solution samples can be reconciled if it is assumed that in the frozen solutions the complex tends to adopt the low-energy (low  $\phi$ ) configuration. A distribution of configurations (with different  $V/\Delta$ 's) could also be masked in the frozen solution measurements since the extraction of  $g$  values is likely to be biased toward the extremes which correspond to maximum values of  $\Delta$ , and in this case minimum values of  $\phi$ .

To the extent that the  $\phi$  dependence of  $V$  can be attributed to pseudo-Jahn-Teller distortion of the porphyrin, this  $\phi$  dependence reflects a Jahn-Teller stabilization of the eclipsed ( $\phi = 0$ ) conformation. This is of particular interest because the  $\phi$  dependence of the total energy has been somewhat difficult to rationalize. Nonbonding repulsion between the imidazole hydrogen atoms and the porphyrin nitrogen atoms, to which the  $\phi$  dependence of the Fe-N<sub>a</sub> distance is attributed, is a maximum at  $\phi = 0$ . Yet as documented by Scheidt and Chipman,<sup>3</sup> most imidazole complexes of metalloporphyrins adopt conformations with small  $\phi$ . While there may be other effects, as proposed by Scheidt and Chipman,<sup>3</sup> that contribute to the relative stability of the  $\phi = 0$  conformation, the present results indicate that pseudo-Jahn-Teller distortion of the porphyrin ligand cannot be ignored in any computation designed to model the  $\phi$  dependence of the total energy.

### Conclusions

EPR observations provide a detailed picture of the changes in electronic structure of ferric porphyrins brought about by changes in axial ligation. In particular, this investigation has demonstrated that rotation of imidazole about the porphyrin normal alters both the spin distribution and the energy of the highest occupied

molecular orbital. In heme protein systems a change in the energy of the highest occupied molecular orbital will affect the reduction potential of the ferric species, while a change in spin distribution may alter the pathway and rate of electron transfer into and out of the iron center. By determining the orientations of the axial and porphyrin ligands the protein may thus exert thermodynamic and kinetic control of the electronically "flexible" heme group.

This investigation has also revealed a significant pseudo-Jahn-Teller contribution to the crystal field, the magnitude of which depends on the orientation of the axial ligands. This orientation dependence is observed in the Fe-N distances of the porphyrin ligand, the magnitude of the rhombic splitting, and the distribution of spin density. A mathematical model of the crystal field that includes effects of axial ligand orientation, pseudo-Jahn-Teller distortion, and trans influence in low-spin ferric porphyrin complexes will be described in the next paper in this series.

**Acknowledgment.** The authors are indebted to the National Institutes of Health (CES GM35329, JSV GM28222) and the National Science Foundation (CES CHE-8340836, JSV CHE-8505473) for financial support, to Dr. Reuel VanAtta for obtaining the polycrystalline EPR spectrum of the tMU complex, and to Prof. Ann Walker and Prof. Robert Scheidt for communication of unpublished results.

**Supplementary Material Available:** Tables of bond lengths, bond angles, interaction distances, atomic positions, and thermal parameters for all atoms (16 pages); listing of observed and calculated structure factors (40 pages). Ordering information is given on any current masthead page.

## Reactions of Iodine with Triphenylphosphine and Triphenylarsine

F. Albert Cotton\* and Piotr A. Kibala

Contribution from the Department of Chemistry and Laboratory for Molecular Structure and Bonding, Texas A&M University, College Station, Texas 77843. Received September 22, 1986

**Abstract:** The reaction of PPh<sub>3</sub> with I<sub>2</sub> leads to disproportionation of iodine and formation of (PPh<sub>3</sub>I)<sup>+</sup> and I<sub>3</sub><sup>-</sup>. Dichloroethane solutions of these give [(PPh<sub>3</sub>I)<sub>2</sub>I<sub>3</sub>]I<sub>3</sub> (**1**) while toluene solutions give (PPh<sub>3</sub>I)<sub>2</sub>I<sub>3</sub> (**2**). Both compounds were structurally characterized by X-ray crystallography. The crystallographic data for **1** are as follows: orthorhombic, space group *Pnma* with unit cell dimensions  $a = 12.517$  (3) Å,  $b = 38.292$  (8) Å,  $c = 9.116$  (3) Å,  $V = 4369$  (3) Å<sup>3</sup>,  $Z = 4$ . The structure was refined to  $R = 0.043$  ( $R_w = 0.049$ ) for 1179 reflections with  $I > 3\sigma(I)$ . The structure of **1** consists of zigzag chains of [(PPh<sub>3</sub>I)<sub>2</sub>I<sub>3</sub>]<sup>+</sup> cations sandwiched in layers of I<sub>3</sub><sup>-</sup> anions. The pertinent crystallographic data for **2** are as follows: monoclinic, space group *P2<sub>1</sub>/n* with unit cell dimensions  $a = 11.583$  (2) Å,  $b = 11.862$  (2) Å,  $c = 15.900$  (3) Å,  $\beta = 95.44$  (2)°,  $V = 2175$  (1) Å<sup>3</sup>,  $Z = 4$ . The structure was refined to  $R = 0.042$  ( $R_w = 0.051$ ) for 2264 reflections with  $I > 3\sigma(I)$ . Molecules of **2** form infinite chains with a distance of 3.741 (1) Å between adjacent ends. The reaction of AsPh<sub>3</sub> with I<sub>2</sub> in dichloroethane gives [(AsPh<sub>3</sub>I)<sub>2</sub>I<sub>3</sub>]I<sub>3</sub> (**3**), which is isostructural with [(PPh<sub>3</sub>I)<sub>2</sub>I<sub>3</sub>]I<sub>3</sub> (**1**).

The discovery of the element iodine, by Bernard Courtois, was reported more than 170 years ago<sup>1a</sup> and the existence<sup>1b</sup> of polyiodides has been known nearly as long. In more recent times it has been recognized that polyiodides exhibit a rich structural chemistry and adopt a variety of geometric arrangements which

depend on the cations with which they are associated.<sup>1c</sup> It was well over a hundred years ago that that commonest of all phosphine ligands, triphenylphosphine, was first described by Michaelis and co-workers.<sup>2</sup>

In view of how widely used both of these substances are, and how omnipresent in inorganic research laboratories, it seems truly astonishing that virtually nothing has been reported<sup>3</sup> concerning

(1) (a) Clement, N.; Desormes, C.-B. *Ann. Chim. Phys.* **1813**, 88, [1], 304. (b) *Gmelins Handbuch der Anorganischen Chemie* [8e Auflage] **1933**, 8, 402-431. (c) Tebbe, K.-F. In *Homocyclic Rings, Chains and Macromolecules*; Rheingold, A. L., Ed.; Elsevier: Amsterdam, 1977; Chapter 24.

(2) (a) Michaelis, A.; Gleichman, L. *Ber. Dtsch. Chem. Ges.* **1882**, 15, 801. (b) Michaelis, A.; Reese, A. *Ibid.* **1882**, 15, 1610.

Table I. Crystal Data for [(PPh<sub>3</sub>I)<sub>2</sub>I<sub>3</sub>]<sub>3</sub> (1)

formula	C <sub>36</sub> H <sub>30</sub> I <sub>8</sub> P <sub>2</sub>
formula wt	1539.8
space group	<i>Pnma</i>
systematic absences	<i>Ok</i> l: $k + l = 2n + 1$ <i>hk</i> 0: $h = 2n + 1$
<i>a</i> , Å	12.517 (3)
<i>b</i> , Å	38.292 (8)
<i>c</i> , Å	9.116 (3)
α, deg	90.0
β, deg	90.0
γ, deg	90.0
<i>V</i> , Å <sup>3</sup>	4369 (3)
<i>Z</i>	4
<i>d</i> <sub>calcd</sub> , g/cm <sup>3</sup>	2.341
crystal size, mm	0.5 × 0.4 × 0.4
μ(Mo Kα), cm <sup>-1</sup>	57.17
data collection instrument	CAD-4
radiation (monochromated in incident beam)	Mo Kα (λ = 0.71073 Å)
orientation reflns, no., range (2θ), deg	25, 12 < 2θ < 25
temp, °C	27
scan method	ω
data col. range, 2θ, deg	4 ≤ 2θ ≤ 50
no. of unique data, total	2289
with $F_o^2 > 3\sigma(F_o^2)$	1179
no. of parameters refined	204
trans. factors, max, min	1.00, 0.94
<i>R</i> <sup>a</sup>	0.043
<i>R</i> <sub>w</sub> <sup>b</sup>	0.049
quality-of-fit indicator <sup>c</sup>	1.219
largest shift/esd, final cycle	0.06
largest peak, e/Å <sup>3</sup>	0.69

<sup>a</sup> $R = \sum ||F_o| - |F_c|| / \sum |F_o|$ . <sup>b</sup> $R_w = [\sum w(|F_o| - |F_c|)^2 / \sum w|F_o|^2]^{1/2}$ ;  $w = 1/\sigma^2(|F_o|)$ . <sup>c</sup>Quality-of-fit =  $[\sum w(|F_o| - |F_c|)^2 / (N_{\text{obsd}} - N_{\text{parameters}})]^{1/2}$ .

their reactions with each other. In fact, as we now report, they react instantly upon being mixed in appropriate solvents such as 1,2-dichloroethane and toluene. Moreover, the structural nature of the resulting crystalline compounds is different for the different solvents and in each case the structures display features that are novel, even in the well-studied area of polyiodide chemistry.

### Experimental Section

**Preparation of [(PPh<sub>3</sub>I)<sub>2</sub>I<sub>3</sub>]<sub>3</sub> (1).** PPh<sub>3</sub> (0.50 g, 1.9 mmol) and I<sub>2</sub> (0.97 g, 3.8 mmol) dissolved in 20 mL of ClCH<sub>2</sub>CH<sub>2</sub>Cl were stirred vigorously for 30 min under an argon atmosphere. The reaction mixture was filtered through Celite. After several days in a refrigerator, red crystals of **1** appeared and were separated. Slow evaporation of the solvent from the mother liquor in the air produced more crystals to give an almost quantitative yield of **1**.

**Preparation of (PPh<sub>3</sub>I)<sub>3</sub> (2).** PPh<sub>3</sub> (0.50 g, 1.9 mmol) and I<sub>2</sub> (0.97 g, 3.8 mmol) dissolved in 20 mL of toluene were refluxed for 30 min under an argon atmosphere. The reaction mixture was allowed to cool and was filtered through Celite to remove an oily residue. After several days in a refrigerator, red crystals of **2** appeared and were separated. The yield was ~10%.

**Preparation of [(AsPh<sub>3</sub>I)<sub>2</sub>I<sub>3</sub>]<sub>3</sub> (3).** AsPh<sub>3</sub> (0.50 g, 1.6 mmol) and I<sub>2</sub> (0.82 g, 3.8 mmol) dissolved in 20 mL of ClCH<sub>2</sub>CH<sub>2</sub>Cl were stirred for 30 min under an argon atmosphere. The reaction mixture was filtered through Celite. After several days in a refrigerator, red crystals appeared and were separated. Slow evaporation of the solvent from the mother liquor in the air produced more crystals to give an almost quantitative yield of **3**. Diffraction photography showed that the crystals had isomorphous unit cell dimensions to those of [(PPh<sub>3</sub>I)<sub>2</sub>I<sub>3</sub>]<sub>3</sub> (**1**).

**X-ray Crystallographic Procedures.** The structures were determined by application of procedures fully described elsewhere.<sup>4</sup> Lorentz, po-

Table II. Crystal Data for (PPh<sub>3</sub>I)<sub>3</sub> (2)

formula	C <sub>18</sub> H <sub>15</sub> I <sub>4</sub> P <sub>1</sub>
formula wt	769.9
space group	<i>P2</i> <sub>1</sub> / <i>n</i>
systematic absences	<i>h</i> 0l: $h + l = 2n + 1$ 0 <i>k</i> 0: $k = 2n + 1$
<i>a</i> , Å	11.583 (2)
<i>b</i> , Å	11.862 (2)
<i>c</i> , Å	15.900 (3)
α, deg	90.0
β, deg	95.44 (2)
γ, deg	90.0
<i>V</i> , Å <sup>3</sup>	2175 (1)
<i>Z</i>	4
<i>d</i> <sub>calcd</sub> , g/cm <sup>3</sup>	2.351
crystal size, mm	0.4 × 0.4 × 0.3
μ(Mo Kα), cm <sup>-1</sup>	57.43
data collection instrument	CAD-4
radiation (monochromated in incident beam)	Mo Kα (λ = 0.71073 Å)
orientation reflns, no., range (2θ), deg	25, 12 < 2θ < 25
temp, °C	27
scan method	ω-2θ
data col. range, 2θ, deg	4 ≤ 2θ ≤ 50
no. of unique data, total	2992
with $F_o^2 > 3\sigma(F_o^2)$	2264
no. of parameters refined	208
trans. factors, max, min	1.00, 0.93
<i>R</i> <sup>a</sup>	0.042
<i>R</i> <sub>w</sub> <sup>b</sup>	0.051
quality-of-fit indicator <sup>c</sup>	1.318
largest shift/esd, final cycle	0.02
largest peak, e/Å <sup>3</sup>	1.04

<sup>a</sup> $R = \sum ||F_o| - |F_c|| / \sum |F_o|$ . <sup>b</sup> $R_w = [\sum w(|F_o| - |F_c|)^2 / \sum w|F_o|^2]^{1/2}$ ;  $w = 1/\sigma^2(|F_o|)$ . <sup>c</sup>Quality-of-fit =  $[\sum w(|F_o| - |F_c|)^2 / (N_{\text{obsd}} - N_{\text{parameters}})]^{1/2}$ .

larization, and absorption corrections were applied to the data.

**Structure of [(PPh<sub>3</sub>I)<sub>2</sub>I<sub>3</sub>]<sub>3</sub> (1).** A crystal of approximate dimensions 0.5 × 0.4 × 0.4 mm was mounted on a CAD-4 diffractometer equipped with graphite monochromated Mo Kα (λ = 0.71073 Å) radiation. The unit cell was indexed on 25 strong reflections in the range 12° ≤ 2θ ≤ 25° selected from a preliminary data collection. Systematic absences *Ok*l ( $k + l = 2n + 1$ ) and *hk*0 ( $h = 2n + 1$ ) indicated *Pnma* or *Pn*2<sub>1</sub>*a* as possible space groups. *Pnma* was confirmed by successful refinement. The positions of the iodine atoms were determined by direct methods program MULTAN-77,<sup>4d</sup> and the remaining atoms were found by iterative applications of least-squares refinement and difference Fourier maps. No attempt was made to include hydrogen atoms in the calculations. Crystal data and experimental details are given in Table I.

**Structure of (PPh<sub>3</sub>I)<sub>3</sub> (2).** A crystal of approximate dimensions 0.4 × 0.4 × 0.3 mm was mounted on a CAD-4 diffractometer equipped with graphite monochromated Mo Kα (λ = 0.71073 Å) radiation. The unit cell was indexed on 25 strong reflections in the range 12° ≤ 2θ ≤ 25°. Systematic absences *h*0l ( $h + l = 2n + 1$ ) and 0*k*0 ( $k = 2n + 1$ ) indicated space group *P2*<sub>1</sub>/*n*. The position of the first iodine atom was determined from a three-dimensional Patterson map, and the remaining atoms were found by iterative application of least-squares refinement and difference Fourier maps. No attempt was made to include hydrogen atoms in the calculations. The final difference synthesis revealed several peaks in the order of 1 eÅ<sup>-3</sup> in the vicinity of the I atoms. The pertinent crystallographic data are summarized in Table II.

### Results and Discussion

**Preparation.** Compounds **1** and **2** were first obtained in small quantities during our investigation of ZrI<sub>4</sub> reactions with phosphines. At first, of course, we presumed them to be triphenylphosphine complexes of zirconium, but it soon became clear that no zirconium was present, and further studies, described below,

(3) (a) The reference by Steinkopf and Schwen (Steinkopf, W.; Schwen, G. *Ber. Dtsch. Chem. Ges.* **1921**, *54*, 1437) contains a passing mention of Ph<sub>3</sub>AsI<sub>2</sub>, which was not characterized. (b) Beveridge and Harris (Beveridge, A. D.; Harris, G. S. *J. Chem. Soc.* **1964**, 6076) report Ph<sub>3</sub>AsI<sub>4</sub> but no characterization thereof besides elemental analysis. (c) Beveridge, Harris, and Inglis (Beveridge, A. D.; Harris, G. S.; Inglis, F. *J. Chem. Soc. A* **1966**, 520) note the existence of "Ph<sub>3</sub>PI<sub>2</sub>" and "Ph<sub>3</sub>PI<sub>4</sub>" and their conductances in CH<sub>2</sub>CN solution. (d) Farhat Ali and Harris (Farhat Ali, M.; Harris, G. S. *J. Chem. Soc., Dalton Trans.* **1980**, 1545) report conductance studies of many "halogen adducts" of Ph<sub>3</sub>P, all with mixed sets of halogens.

(4) (a) Bino, A.; Cotton, F. A.; Fanwick, P. E. *Inorg. Chem.* **1979**, *18*, 3558. (b) Cotton, F. A.; Ferez, B. A.; Deganello, G.; Shaver, A. J. *J. Organomet. Chem.* **1973**, *50*, 227. (c) All calculations were performed with the Enraf-Nonius Structure Determination Package on the Vax 11/80 computer at the Department of Chemistry, Texas A&M University, College Station, TX 77843. (d) Main, P.; Wolfson, M. M.; Lessinger, L.; Germain, G.; Declercq, J. P. MULTAN-77, A System of Computer Programs for the Automatic Solution of Crystal Structures from X-ray Diffraction Data. Universities of York, England and Louvain, Belgium, 1977.

**Table III.** Atomic Positional Parameters and Equivalent Isotropic Displacement Parameters ( $\text{\AA}^2$ ) and Their Estimated Standard Deviations for  $[(\text{PPh}_3)_2\text{I}_3]^+$  (**1**)

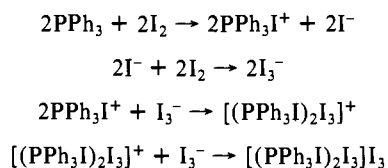
I(1)	0.500	0.500	0.500	5.16 (5)
I(2)	0.2857 (2)	0.47282 (4)	0.4551 (2)	7.51 (5)
I(3)	0.5062 (2)	0.250	0.1681 (2)	6.12 (6)
I(4)	0.6417 (2)	0.250	0.4150 (3)	5.45 (6)
I(5)	0.7875 (2)	0.250	0.6862 (3)	5.81 (6)
I(6)	0.9759 (1)	0.18224 (4)	0.6801 (2)	4.86 (3)
P(1)	1.1040 (5)	0.1358 (1)	0.6640 (6)	3.9 (1)
C(11)	1.044 (2)	0.0986 (5)	0.580 (2)	4.2 (5)
C(12)	1.060 (2)	0.0942 (5)	0.426 (2)	4.9 (6)
C(13)	1.010 (2)	0.0646 (5)	0.361 (2)	5.3 (5) <sup>a</sup>
C(14)	0.950 (2)	0.0416 (5)	0.449 (2)	4.9 (6)
C(15)	0.935 (2)	0.0484 (6)	0.599 (2)	5.3 (6)
C(16)	0.982 (2)	0.0774 (5)	0.664 (2)	5.1 (5)
C(21)	1.216 (1)	0.1486 (5)	0.562 (2)	2.9 (4)
C(22)	1.226 (1)	0.1821 (5)	0.502 (2)	4.2 (5)
C(23)	1.317 (2)	0.1903 (6)	0.415 (2)	5.8 (6)
C(24)	1.400 (2)	0.1672 (6)	0.398 (2)	5.0 (6)
C(25)	1.388 (2)	0.1316 (6)	0.458 (2)	4.8 (5)
C(26)	1.300 (2)	0.1229 (5)	0.543 (2)	4.0 (5)
C(31)	1.149 (2)	0.1242 (5)	0.847 (2)	4.0 (5)
C(32)	1.176 (2)	0.1528 (6)	0.936 (2)	5.2 (6)
C(33)	1.216 (2)	0.1457 (5)	1.079 (3)	5.8 (6)
C(34)	1.236 (2)	0.1111 (6)	1.117 (2)	5.3 (6)
C(35)	0.710 (2)	0.0820 (6)	0.468 (2)	4.7 (5)
C(36)	1.165 (2)	0.0887 (5)	0.885 (2)	4.7 (5) <sup>a</sup>

<sup>a</sup>These atoms were refined isotropically. Anisotropically refined atoms are given in the form of the isotropic equivalent thermal parameter defined as  $\frac{1}{3}[a^2\beta_{11} + b^2\beta_{22} + c^2\beta_{33} + ab(\cos \gamma)\beta_{12} + ac(\cos \beta)\beta_{13} + bc(\cos \alpha)\beta_{23}]$ .

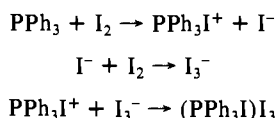
revealed their composition and structure. It seems remarkable that even if no one ever observed the formation of these compounds by direct reaction of iodine with triphenylphosphine, neither did anyone ever report (so far as we have been able to find) that they could arise by reaction of triphenylphosphine, that ubiquitous ligand, with some metal iodide.

We were soon able to show that **1** and **2** could be synthesized directly by reaction of  $\text{PPh}_3$  with  $\text{I}_2$ . Two moles of  $\text{I}_2$  react easily at room temperature with one mole of  $\text{PPh}_3$  in dichloroethane. The crystalline product can be obtained in almost quantitative yield by slow evaporation of the solvent. The reaction product was structurally characterized by X-ray crystallography and identified as  $[(\text{PPh}_3)_2\text{I}_3]^+$  (**1**).

The formation of  $[(\text{PPh}_3)_2\text{I}_3]^+$  (**1**) could proceed according to the following scheme:

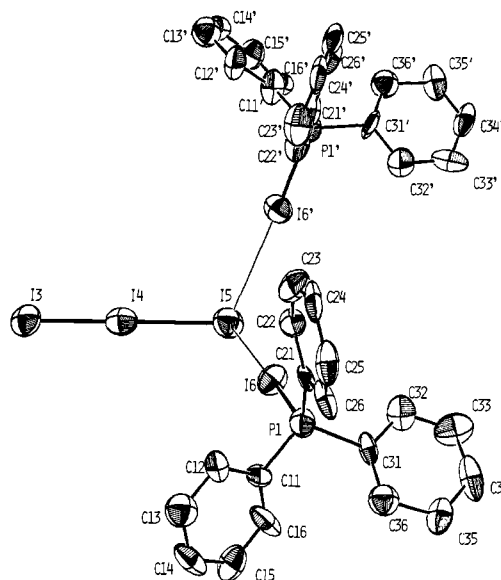


The reaction of  $\text{PPh}_3$  and  $\text{I}_2$  in toluene gives a different product than the one in dichloroethane. The yield of the product, identified by X-ray crystallography as  $(\text{PPh}_3\text{I})\text{I}_3$  (**2**), is low. The formation of  $(\text{PPh}_3\text{I})\text{I}_3$  (**2**) could proceed according to the following scheme:

**Table IV.** Selected Bond Distances in Angstroms and Bond Angles in Degrees for  $[(\text{PPh}_3)_2\text{I}_3]^+$  (**1**)<sup>a</sup>

I(1)–I(2)	2.906 (2)	I(3)–I(4)	2.819 (3)	I(4)–I(5)	3.073 (3)
I(5)–I(6)	3.506 (2)	I(6)–P(1)	2.401 (5)	P(1)–C(11)	1.78 (2)
P(1)–C(21)	1.76 (2)	P(1)–C(31)	1.82 (2)		
I(2)–I(1)–I(2')	180.00 (0)	I(3)–I(4)–I(5)	179.4 (1)		
I(4)–I(5)–I(6)	112.74 (6)	I(6)–I(5)–I(6')	95.48 (7)		
I(5)–I(6)–P(1)	177.4 (2)	I(6)–P(1)–C(11)	109.6 (8)		
I(6)–P(1)–C(21)	111.1 (7)	I(6)–P(1)–C(31)	109.5 (7)		

<sup>a</sup>Numbers in parentheses are estimated standard deviations in the least significant digits.

**Figure 1.** ORTEP drawing of  $[(\text{PPh}_3)_2\text{I}_3]^+$  cation of  $[(\text{PPh}_3)_2\text{I}_3]\text{I}_3$  (**1**) with the atom labeling scheme. Atoms are represented by their ellipsoids at the 50% probability level.

**Structures.**  $[(\text{PPh}_3)_2\text{I}_3]^+$  (**1**). The structure of  $[(\text{PPh}_3)_2\text{I}_3]^+$  (**1**) consists of parallel zigzag chains of  $[(\text{PPh}_3)_2\text{I}_3]^+$  cations sandwiched between layers of  $\text{I}_3^-$  anions. The structure of the  $[(\text{PPh}_3)_2\text{I}_3]^+$  cation of  $[(\text{PPh}_3)_2\text{I}_3]\text{I}_3$  (**1**) is shown in Figure 1, which also explains the labeling scheme. The atomic positional parameters and equivalent isotropic parameters are presented in Table III. Selected bond distances and angles are collected in Table IV. The  $[(\text{PPh}_3)_2\text{I}_3]^+$  cation may be viewed as consisting of two  $(\text{PPh}_3\text{I})^+$  fragments related to each other by the plane of symmetry containing the  $\text{I}_3^-$  moiety. The triiodide fragment is nearly linear, the I(3)–I(4)–I(5) angle being  $179.4 (1)^\circ$ , and has distinctly unequal bond lengths, I(3)–I(4) =  $2.819 (3) \text{ \AA}$  and I(4)–I(5) =  $3.073 (3) \text{ \AA}$ . The degree of asymmetry, i.e., the difference between the two I–I distances, is  $0.254 (4) \text{ \AA}$  and is caused by an electrostatic interaction between the I(5) atom of  $\text{I}_3^-$  and the I(6) atoms of two  $(\text{PPh}_3\text{I})^+$  fragments. The I(5)–I(6) distance of  $3.506 (2) \text{ \AA}$  indicates a very strong van der Waals interaction that justifies viewing the  $[(\text{PPh}_3)_2\text{I}_3]^+$  as one entity.

The  $[(\text{PPh}_3)_2\text{I}_3]^+$  cations form a network of parallel zigzag chains sandwiched between layers of isolated  $\text{I}_3^-$  anions (Figure 2). The interactions between adjacent cations in the chain are very weak as indicated by longer distances (I(5)–I(3') =  $4.233 (3) \text{ \AA}$ , I(6)–I(3') =  $4.117 (2) \text{ \AA}$ ) which are close to  $\sim 4.3 \text{ \AA}$ , the sum of the van der Waals radii. The isolated triiodide anions that form a layered structure in the lattice occupy centers of inversion and have an I–I distance of  $2.906 (2) \text{ \AA}$ . The packing of the molecule is shown in Figure 3.

Although there is now a vast literature on the structures of triiodide compounds, compound **1** appears to be unique in two ways. First, it is the only one to contain both symmetrical and unsymmetrical  $\text{I}_3^-$  ions. The symmetrical  $\text{I}_3^-$  ions here, as in all other cases where they have been observed, reside on crystallographic inversion centers, and thus the linearity and equality of I–I distances is rigorous. The unsymmetrical ones are, as usual, nearly linear, but they have distinctly different I–I distances. The difference,  $0.254 (4) \text{ \AA}$ , is large, but short of the largest one known,

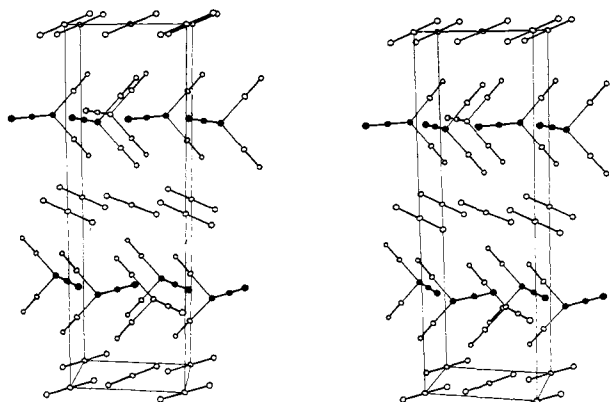


**Figure 2.** A stereopair depicting zigzag chains of [(PPh<sub>3</sub>I)<sub>2</sub>I<sub>3</sub>]<sup>+</sup> cations in the unit cell of [(PPh<sub>3</sub>I)<sub>2</sub>I<sub>3</sub>]I<sub>3</sub> (**1**). Carbon atoms of the phenyl rings are omitted for clarity. Iodine atoms of I<sub>3</sub><sup>-</sup> fragment in [(PPh<sub>3</sub>I)<sub>2</sub>I<sub>3</sub>]<sup>+</sup> are darkened to show the zigzag structure. Orientation of axes: *a*, across; *b*, down; *c*, toward viewer.

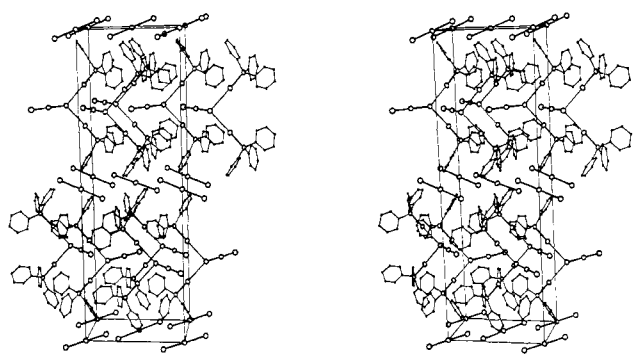


**Figure 3.** A stereopair depicting the unit cell packing for [(PPh<sub>3</sub>I)<sub>2</sub>I<sub>3</sub>]I<sub>3</sub> (**1**). The axes are oriented as in Figure 2.

**Table V.** Atomic Positional Parameters and Equivalent Isotropic Displacement Parameters (Å<sup>2</sup>) and Their Estimated Standard Deviations for (PPh<sub>3</sub>I)I<sub>3</sub>, (**2**)<sup>a</sup>

I(1)	0.37690 (8)	-0.28381 (8)	-0.19762 (5)	4.14 (2)
I(2)	0.55159 (7)	-0.22537 (7)	-0.05285 (4)	3.40 (2)
I(3)	0.71509 (9)	-0.17944 (9)	0.08915 (5)	5.67 (2)
I(4)	0.48467 (8)	-0.01683 (7)	-0.25414 (5)	3.93 (2)
P(1)	0.6280 (3)	0.1208 (2)	-0.2807 (2)	2.65 (6)
C(11)	0.7150 (9)	0.1498 (9)	-0.1844 (6)	2.8 (2)
C(12)	0.821 (1)	0.207 (1)	-0.1891 (7)	3.7 (3)
C(13)	0.889 (1)	0.239 (1)	-0.1151 (7)	3.9 (3)
C(14)	0.847 (1)	0.215 (1)	-0.0366 (7)	4.2 (3)
C(15)	0.743 (1)	0.158 (1)	-0.0321 (7)	4.5 (3)
C(16)	0.673 (1)	0.124 (1)	-0.1065 (7)	3.9 (3)
C(21)	0.711 (1)	0.0622 (9)	-0.3581 (6)	3.0 (2)
C(22)	0.665 (1)	0.064 (1)	-0.4434 (7)	4.0 (3)
C(23)	0.729 (1)	0.010 (1)	-0.5029 (7)	4.7 (3)
C(24)	0.664 (1)	0.458 (1)	-0.0216 (8)	4.6 (3)
C(25)	0.875 (1)	-0.048 (1)	-0.3950 (8)	4.4 (3)
C(26)	0.816 (1)	0.0044 (9)	-0.3337 (7)	3.4 (2)
C(31)	0.562 (1)	0.2497 (8)	-0.3196 (6)	2.7 (2)
C(32)	0.459 (1)	0.2876 (9)	-0.2883 (7)	3.7 (3)
C(33)	0.417 (1)	0.393 (1)	-0.3133 (8)	4.3 (3)
C(34)	0.475 (1)	0.460 (1)	-0.3652 (7)	3.9 (3)
C(35)	0.577 (1)	0.4219 (9)	-0.3967 (7)	3.3 (2)
C(36)	0.623 (1)	0.3179 (9)	-0.3734 (7)	3.0 (2)

<sup>a</sup> Anisotropically refined atoms are given in the form of the isotropic equivalent thermal parameter defined as  $\frac{4}{3}[a^2\beta_{11} + b^2\beta_{22} + c^2\beta_{33} + ab(\cos\gamma)\beta_{12} + ac(\cos\beta)\beta_{13} + bc(\cos\alpha)\beta_{23}]$ .

which is in NH<sub>4</sub>I<sub>3</sub> (0.322 (6) Å).<sup>5</sup> What is particularly interesting here is that we can identify a very specific set of interactions that are responsible for the difference in bond lengths, whereas in the

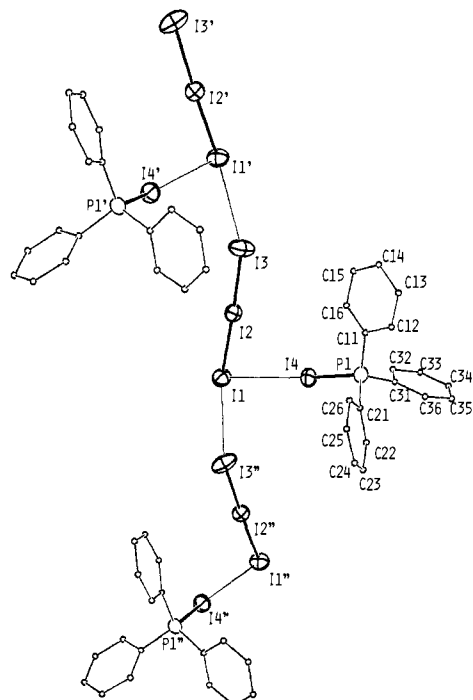


**Figure 4.** ORTEP drawing of (PPh<sub>3</sub>I)I<sub>3</sub> (**2**) with the atom labeling scheme. The two adjacent molecules are also included to show the chain structure of (PPh<sub>3</sub>I)I<sub>3</sub>. Carbon atoms of the phenyl rings are represented by arbitrarily tiny spheres for clarity. All other atoms are represented by their ellipsoids at the 50% probability level.

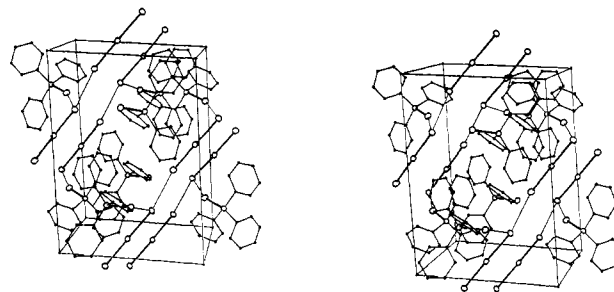


**Figure 5.** A stereopair depicting the unit cell packing for (PPh<sub>3</sub>I)I<sub>3</sub> (**2**). Orientation of axes: *a*, across; *c*, down; *b*, toward viewer.

other case it is not clear why a packing arrangement leading to a more symmetrical structure could not have been found. We see here the close approach of two PPh<sub>3</sub>I<sup>+</sup> iodine atoms to one end of the unsymmetrical I<sub>3</sub><sup>-</sup> ion. This, quite logically, leads to a polarization of the type shown in eq 1, with a resultant lengthening of one I-I bond.



(PPh<sub>3</sub>I)I<sub>3</sub> (**2**). An ORTEP drawing of (PPh<sub>3</sub>I)I<sub>3</sub> (**2**) is shown in Figure 4, which also explains the labeling scheme. The atomic positional parameters and equivalent isotropic parameters are presented in Table V. Selected bonds distances and angles are collected in Table VI. The "molecule" of (PPh<sub>3</sub>I)I<sub>3</sub> (**2**) arises from the strong interaction of a I<sub>3</sub><sup>-</sup> anion and a (PPh<sub>3</sub>I)<sup>+</sup> cation. The distance between the terminal iodine atom of I<sub>3</sub><sup>-</sup> and the iodine atoms of (PPh<sub>3</sub>I)<sup>+</sup>, I(1)-I(4) = 3.551 (1) Å, is slightly longer than the corresponding interaction in [(PPh<sub>3</sub>I)<sub>2</sub>I<sub>3</sub>]I<sub>3</sub> (**1**) but not inconsistent with the treatment of (PPh<sub>3</sub>I)I<sub>3</sub> as one unit. The triiodide fragment is nearly linear, the I(1)-I(2)-I(3) angle being 177.23 (4), and has a moderately asymmetric bond length distribution, I(1)-I(2) = 2.998 (1) Å and I(2)-I(3) = 2.858 (1) Å. That difference between the two I-I distances  $\Delta = 0.140$  (1) Å, much less than that found in [(PPh<sub>3</sub>I)<sub>2</sub>I<sub>3</sub>]I<sub>3</sub> (**1**), is easily explained. In **1** the terminal iodine atom of the I<sub>3</sub><sup>-</sup> fragment of the

(5) (a) Cheeseman, G. H.; Finney, A. I. T. *Acta Crystallogr.* **1972**, *B28*, 1331. (b) Tebbe, K.-F.; Freckmann, B.; Hoerner, M.; Hiller, W.; Straehle, J. *Acta Crystallogr.* **1985**, *C41*, 660.

**Table VI.** Selected Bond Distances in Angstroms and Bond Angles in Degrees for  $(\text{PPh}_3\text{I})_3$ , (**2**)<sup>a</sup>

I(1)–I(2)	2.998 (1)	I(1)–I(3')	3.741 (1)	I(1)–I(4)	3.551 (1)
I(2)–I(3)	2.858 (1)	I(4)–P(1)	2.395 (3)	P(1)–C(11)	1.786 (9)
P(1)–C(21)	1.775 (10)	P(1)–C(31)	1.794 (9)		
I(2)–I(1)–I(3')	165.11 (3)	I(1)–I(4)–P(1)	156.79 (7)		
I(2)–I(1)–I(4)	76.13 (2)	I(4)–P(1)–C(11)	108.9 (3)		
I(1)–I(2)–I(3)	177.23 (4)	I(4)–P(1)–C(21)	106.7 (4)		
I(1')–I(3)–I(2)	158.63 (4)	I(4)–P(1)–C(31)	111.2 (4)		

<sup>a</sup>Numbers in parentheses are estimated standard deviations in the least significant digits.

$[(\text{PPh}_3)_2\text{I}_3]^+$  cation interacts with two  $(\text{PPh}_3\text{I})^+$  fragments while in **2** the terminal iodine atom of  $\text{I}_3^-$  interacts with only one  $(\text{PPh}_3\text{I})^+$ . Molecules of  $(\text{PPh}_3\text{I})_3$  (**2**) interact strongly with each other, as shown by the distance of 3.741 (1) Å between adjacent  $\text{I}_3^-$  ions (Figure 4). They form a network of parallel infinite chains in which successive units in the chain are related by the  $2_1$  symmetry axis (Figure 5).

Another interesting and novel feature of this chemistry is the formation of the  $\text{PPh}_3\text{I}^+$  ion. In both **1** and **2** the  $\text{PPh}_3\text{I}^+$  fragments are nearly identical. The average P–I bond length of 2.398 (3) Å compares favorably with the value of 2.43 (4) Å found in  $\text{PI}_3^6$  and indicates strong covalent bonding. The  $\text{PPh}_3\text{I}^+$  ion belongs to the more general class of  $\text{PR}_n\text{X}_{4-n}^+$  phosphonium cations. Examples of those include the following:  $\text{PCl}_4^+$  in  $(\text{PCl}_4)(\text{PCl}_6)^7$ ,  $\text{PBr}_4^+$  in  $(\text{PBr}_4)\text{Br}^8$ ,  $\text{PETCl}_3^+$  in  $(\text{PETCl}_3)(\text{AlCl}_4)^9$ ,  $\text{PR}_2\text{Cl}_2^+$  in  $(\text{PR}_2\text{Cl}_2)\text{Cl}$  where R = Me, Et, and  $\text{PR}_3\text{Cl}^+$  in  $(\text{PR}_3\text{Cl})\text{Cl}$  where R = Ph, Me, Et.<sup>10</sup> The first two were structurally characterized by X-ray crystallography. The P–Cl bond distance in the  $\text{PCl}_4^+$  ion is 1.98 Å compared with 2.2 Å in  $\text{PBr}_4^+$  and 2.398 (3) Å in  $\text{PPh}_3\text{I}^+$ . We believe that our  $(\text{PPh}_3\text{I})^+$  is the first structurally characterized iodophosphonium ion.

The phosphine compounds reported here should be compared with the well-known amine complexes of  $\text{I}^+$ , especially those with pyridine and its derivatives.<sup>11</sup> These have traditionally—and probably correctly—been considered as containing cationic iodine stabilized by coordination. We believe that the  $\text{PPh}_3\text{I}^+$  ion, re-

ported here for the first time, is best regarded as a novel example of a phosphonium ion, in which the positive charge resides largely on the phosphorus atom and the four bonds to the phosphorus atom are all essentially covalent, single bonds. It may be noted in support of this view that the subtraction of the covalent radius for an  $\text{sp}^2$  hybridized carbon atom (0.75 Å) from the mean of the P–C bond lengths gives 1.04 Å, while the subtraction of the covalent radius of iodine (1.33 Å) from the mean P–I distance gives nearly the same result, viz., 1.07 Å.

**Concluding Remarks.** Both **1** and **2** have the same empirical formula. However, they are different structurally. The difference in the structures cannot be simply explained by the presence of solvent molecules in the lattice, since there are none in either. Apparently the polarity of the solvent determines the type of the structure. In more polar dichloroethane  $[(\text{PPh}_3)_2\text{I}_3]\text{I}_3$  (**1**) is preferred (with clear separation between anions and cations). In less polar toluene  $(\text{PPh}_3\text{I})_3$  (**2**) is formed where anions strongly interact with cations. This phenomenon of a compound adopting two distinctly different structures when crystallized from two different solvents, even though solvent molecules are not a part of either crystal structure, also has no precedent, so far as we can ascertain. If not actually unprecedented it is surely extremely rare.

We have also shown that  $\text{AsPh}_3$  reacts with  $\text{I}_2$  in dichloroethane in a manner similar to that of  $\text{PPh}_3$ . The reaction product,  $[(\text{AsPh}_3)_2\text{I}_3]\text{I}_3$  (**3**), was shown to be isostructural with  $[(\text{PPh}_3)_2\text{I}_3]\text{I}_3$  (**1**).

**Acknowledgment.** We thank Dr. Willi Schwotzer for helpful discussions and the Robert A. Welch Foundation for support.

**Supplementary Material Available:** Full listing of bond distances bond angles, and isotropic equivalent displacement parameters (6 pages); listing of observed and calculated structure factors (18 pages). Ordering information is given on any current masthead page.

(6) Allen, P. W.; Sutton, L. E. *Acta Crystallogr.* **1950**, *3*, 46.

(7) (a) Clark, D.; Powell, H. M.; Wells, A. F. *J. Chem. Soc.* **1942**, 642.

(b) Powell, H. M.; Clark, D.; Wells, A. F. *Nature (London)* **1940**, *145*, 149.

(8) (a) Powell, H. M.; Clark, D. *Nature (London)* **1940**, *145*, 971. (b) van Driel, M.; MacGillavry, C. H. *Recl. Trav. Chim.* **1943**, *62*, 167.

(9) Payne, D. S. *Top. Phosphorus Chem.* **1967**, *4*, 103 and references therein.

(10) Greenwood, N. N.; Earnshaw, A. *Chemistry of the Elements*; Pergamon: New York, 1984; p 573 and references therein.

(11) Hassel, O.; Hope, H. *Acta Chem. Scand.* **1961**, *15*, 407.